JOURNAL OF MATERIALS SCIENCE 30 (1995) 5825–5832

Characterization of shock-hardened Al-8090 alloy

R. ESQUIVEL, O. T. INAL
Materials and Metallurgical Engineering Department, New Mexico Institute of Mining and Technology, Socorro, NM 87801, USA

The structure and mechanical properties of Al–Li8090 alloy, that was dynamically deformed and then age hardened, were studied as a function of the changes in the nature and amount of precipitates produced. A comparison was made between two groups of samples, one group that was solution heat treated (SHT) and quenched from 530 °C before the dynamic deformation and the other group that was dynamically deformed in the as-received (AR) condition. The higher values for microhardness and ultimate tensile strength observed (138 and 140 VHN, and 405 and 458 MPa, respectively), subsequent to shock treatment (ST), have been attributed to the increase in dislocation density and grain-boundary precipitation produced due to shock deformation. Dislocations and grain boundaries were assumed to act as precipitation sites and an increase in dislocation density, due to ST, was expected to increase precipitation density of $\delta'(Al_3Li)$, $S(Al_2CuMg)$, and $T_1(Al_2CuLi)$ phases which, in turn, are expected to increase strength properties of the alloy. Differential scanning calorimetry showed that, for the species that precipitate below 180 °C, $\delta'(Al_3Li)$ and GP zones, an increase in the amount of deformation increased the precipitation temperatures. However, for the species that precipitate at 197 °C, $S(Al_2CuMg)$, an increase in the amount of deformation produced a decrease in its precipitation temperature. These results have been partially confirmed by the activation energy calculations for temperatures below 197 °C, which show a decrease of precipitation energies with an increase in the amount of deformation. Activation energies calculated from ageing curves showed that when ageing at low temperature (165–180 °C range), activation energies for the precipitation process are decreased upon increase in cold work. Shock treatment of SHT samples exhibited decreased activation energy values of precipitation, from 36.14 kcal mol^{-1} for the SHT sample to 24.18, 24.08, and 21.00 kcal mol^{-1} for SHT + ST samples 1, 2, and 3, respectively (corresponding to 1, 2, and 3 sheets of explosive). Activation energies of precipitation for AR + ST samples showed even lower values; 9.45, 9.95, and 8.21 kcal mol^{-1} for samples 4, 5, and 6, respectively. These activation energies strongly corroborate the role of defect substructure on the age-hardening kinetics of this alloy.

1. Introduction

Aluminium alloys containing up to 3 wt % lithium are currently being developed for aerospace applications because of their low density and high strength when compared to more conventional aluminium alloys such as 2024 and 7075. In particular, Al-8090 alloy (Al–Li–Cu–Mg–Zr) exhibits a 15% increase in strength and about 10% decrease in density in comparison to the above-mentioned alloys [1].

The main strengthening phase in the latter alloy is the intermetallic Al_3Li which has an ordered $L1_2$ structure. However, the presence of this phase within the matrix produces planar slip (due to its shearable nature) and increases stress concentrations at high-angle grain boundaries. In addition, large, quasi-equilibrium phases are precipitated at high-angle grain boundaries when Al_3Li precipitate-free zones (PFZ) are formed. These two factors reduce grain-boundary strength and decrease toughness [2].

The most practical method to improve toughness is to modify the grain-boundary precipitation during the ageing treatment. Copper and magnesium are added to this alloy to form two other intermetallics, $S(Al_2CuMg)$ and $T_1(Al_2CuLi)$. These precipitates inhibit the occurrence of planar slip (because of their non-shearable nature which tends to promote cross slip) and, consequently, diminish stress concentration at the grain boundaries. The $S(Al_2CuMg)$ phase precipitates preferentially on dislocations and subgrain boundaries. Straining prior to ageing increases the number of dislocations and therefore increases the $S(Al_2CuMg)$ precipitation [3].

The present work studies the effect of the application of high strain rates to the A1-8090 alloy to increase dislocation density and verify the latter role in this precipitation process.

0022–2461

2. Experimental procedure

2.1. Shock treatment and sample preparation

The Al-8090 alloy used in the present study was supplied by Alcoa under 8090-F designation. This designation indicates the alloy to be in the as-fabricated condition, though no control on the amount of strain hardening in this fabrication procedure is indicated to exist. Six samples of this alloy were embedded into an aluminium (Al-1100) block that was machined to a very fine finish; this procedure causes shock waves to pass through the block, rather than being reflected at the sample/support interface with a change in sign. The sample dimensions used were 3 in by 2 in by 1 in (~ 7.62 cm $\times$ 5.08 cm $\times$ 2.54 cm). Samples 1, 2, and 3 were solution heat treated (SHT) at 530 °C for 1 h, and samples 4, 5, and 6 were kept in the as-received (AR) condition corresponding to an extruded microstructure; the arrangement of samples with the above designation is shown in Fig. 1. The distance between the individual samples and the samples and edges of the support block was kept to 2 in (~ 5.08 cm) to avoid spalling.

Explosive sheets of Dupont Deta Sheet C-1 were laid down on top of this arrangement. The C-1 explosive has a composition of 91% RDX ($C_3H_6N_6O_6$), 2.1% rubber, 1.6% oil, and 5.3% plasticizer, and a detonation velocity of 8.0 km s^{-1} [4]. Samples 1 and 4 were covered with one sheet, samples 2 and 5 were covered with two sheets and samples 3 and 6 were covered with three sheets of explosive. Increased thickness of the explosive was assumed to correspond to a commensurate increase in the pulse duration of the shock wave [5].

2.2. Structural and mechanical property evaluation

After shock treatment, samples were carefully cut and polished for differential scanning calorimetry (DSC) analysis. A total of 12 samples from the set, plus 2 samples in the as-received condition, plus 2 samples in the as-received + solution heat-treated condition were analysed on a Perkin–Elmer DSC 1700 system. The heating rate was 10 °C min^{-1}, over a temperature range of 50–450 °C. The temperatures where the endothermic or exothermic reactions occurred were determined.

Solution heat treatment as well as the age-hardening heat treatments were all performed in a General Signal Linderberg 58434 furnace. Solution treatment was done at 530 °C for 1 h.

Age-hardening temperatures were selected from the results of DSC analysis, and they are as follows: 165 °C for the precipitation of Guinier–Preston (GP) zones, 180 and 197 °C for the precipitation of δ′(Al_3Li), and 260 °C for the precipitation of S(Al_2CuMg).

In all cases, samples were taken out of the furnace every 1/2 h for the first 2 h and then every 4 h until the ageing treatment was complete. From the set of six samples that were aged, samples 1, 2, and 3 had been solution heat treated, while samples 4, 5, and 6 were in the as-received condition.

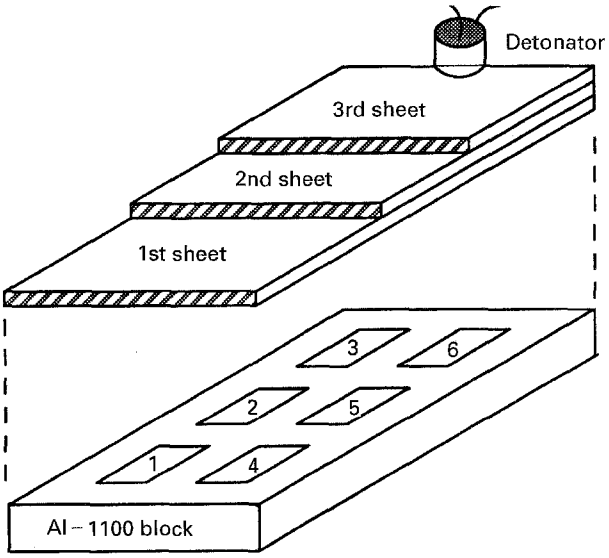

Figure 1 Sample arrangement prior to shock treatment.

Microhardness testing was done on all samples after quenching from the age-hardening treatment. Measurements were made on a Leco M-400 hardness tester with a load of 0.2 kg applied for 15 s. Five measurements were made for each sample and then the standard deviation was calculated. Previous to the measurements, final polishing was performed on each sample to remove oxides and any other impurities produced during the heat treatment.

As a result, 48 curves (VHN against time) were made and used to determine the activation energies for the precipitation during the ageing of the Al-8090 alloy as a function of pressure, pulse duration, ageing temperature and time.

Peak-aged samples were prepared for tensile testing. The standard sizes given in ASTM B557M were followed as closely as possible (due to limitation of the samples sizes). The average measurements of the tensile test samples were 0.15 cm thick, 0.63 cm wide and 2.15 cm gauge length. Tests were performed on an Instron 1122 Tensometer at a strain rate of 4.23×10^{-6} m s^{-1}.

3. Results and discussion

3.1. Differential scanning calorimetry

Fig. 2 shows a plot that corresponds to sample 4 which was in the AR condition and had one sheet of explosive. Previous studies on the precipitation kinetics of Al-8090 alloy [6, 7] have shown the first endothermic peak to correspond to the formation of GP zones. The second endothermic peak can be resolved into two peaks, one attributed to the beginning of δ′(Al_3Li) dissolution and the other attributed to the formation of S(Al_2CuMg). The third endothermic peak is due to complete dissolution of the precipitated phases. Likewise, the first endothermic peak is said to correspond to the formation of δ′(Al_3Li) and the second exothermic peak is attributed to the beginning of dissolution of S(Al_2CuMg) and the formation of δ(AlLi).

Three of the peaks are of great interest in the present study because they correspond to the precipitation of

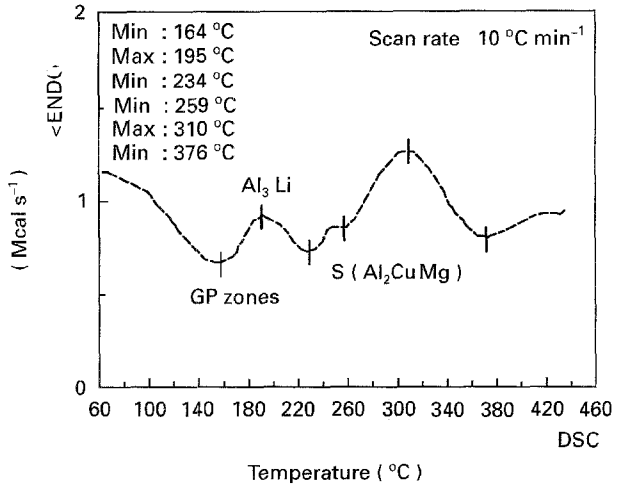

Figure 2 Typical DSC plot. This particular plot corresponds to sample 4, which was in the AR condition and had one sheet of the explosive.

TABLE I Precipitation temperatures of the three precipitates of interest

	Precipitation temperature (°C)		
	GP zones	$\delta'(Al_3Li)$	$S(Al_2CuMg)$
SHT	111 ± 5	150 ± 6	263 ± 1
1, 2, 3 (SHT + ST)	116 ± 4	180 ± 2	258 ± 3
AR	158 ± 1	190 ± 1	264 ± 1
4, 5, 6 (AR + ST)	165 ± 3	197 ± 3	258 ± 3

TABLE II Summary of the time to peak age from the respective ageing plots

Sample	Peak ageing time (h)		
	165 °C	180 °C	197 °C
1	116	67	8
3	60	40	8
4	83	58	8
6	50	25	8
SHT	833	166	50

$\delta'(Al_3Li)$, $S(Al_2CuMg)$, and the GP zones. Table I shows that the temperatures at which GP zones and the $\delta'(Al_3Li)$ phase precipitate change drastically, depending on the metallurgical condition of the sample previous to the shock treatment. The same is true for $S(Al_2CuMg)$ precipitation, but to a lesser degree.

Precipitation of GP zones takes place at 111 °C in the SHT sample and at 158 °C in the AR sample. In the case of the samples that were shock treated (ST), precipitation of GP zones takes place at 116 °C for samples 1, 2, and 3 (SHT + ST) and at 165 °C for samples 4, 5, and 6 (AR + ST).

Precipitation of $\delta'(Al_3Li)$ takes place at 150 °C for the SHT sample and at 190 °C for the AR sample. In the case of ST samples, $\delta'(Al_3Li)$ precipitates at 180 °C for samples 1, 2, and 3 and at 197 °C for samples 4, 5, and 6.

Table I also shows that changes in pulse duration do not change precipitation temperature. That is, for each precipitate in samples 1, 2, and 3, the same precipitation temperature is observed. The same is true for samples 4, 5, and 6 as well. This evidence suggests the shortest pulse duration utilized to be of sufficient magnitude for the creation of a uniform defect substructure throughout the sample cross-section. The uniform microhardness values obtained for all sample cross-sections also lend support to this claim.

Higher temperatures are required for the precipitation of GP zones and $\delta'(Al_3Li)$ phase in Al-8090 alloy, as the amount of previous cold work given to the sample is increased. This increase is shown in Table II, where the precipitation temperature for GP zones of the SHT sample (111 °C), with no cold work, is compared to the AR sample (158 °C), which had cold work from the fabrication process. When the samples are shock treated, i.e. further cold work applied to them, the precipitation temperature is seen to increase even further: from 111 °C to 116 °C in the case of the SHT samples and from 158 °C to 165 °C in the case of the AR samples. The same trend is observed for the precipitation of the $\delta'(Al_3Li)$ phase; precipitation temperatures increased from 150 °C to 180 °C in the SHT and from 190 °C to 197 °C in the AR samples upon shock treatment.

The precipitation of the $S(Al_2CuMg)$ phase shows different behaviour from those detailed above. First, the pre-shock-treatment condition does not seem to affect its precipitation temperature. The SHT samples, as well as the AR samples, both exhibit precipitation of this phase at 263 °C. Second, when these samples are shock treated, the precipitation temperature is reduced (opposite to the behaviour shown by GP zones and $\delta'(Al_3Li)$ phase), from 264 °C to 258 °C.

A reduction of the $S(Al_2CuMg)$ precipitation temperature is beneficial from a processing point of view. Because the temperature for the ageing treatment is lowered, this lower temperature reduces the chance for the formation of the δ(AlLi) phase in the peak-aged and over-aged conditions. The δ(AlLi) is known to precipitate at high-angle grain boundaries, promoting the formation of precipitate-free zones (PFZ) which, in turn, reduces fracture toughness for these materials [8, 9] ; thus its elimination is very desirable.

The fact that no changes in precipitation temperatures were detected upon change in pulse duration may be explained in terms of the saturation of dislocation density even at the lowest pulse duration (one sheet of explosive) utilized in the present study; thus an increase in pulse duration contributed little to precipitation kinetics in Al-8090 alloy, as also verified elsewhere [10].

3.2. Ageing heat treatment

When samples are shock treated, the general trend is that the time to peak is reduced considerably for both SHT and AR samples. Table II shows that sample 1 (SHT + 1 sheet) required 116 h to peak age at 165 °C (compared to 833 h for the SHT sample), and sample 3 (SHT + 3 sheets) required only 60 h to peak age. Sample 4 (AR + 1 sheet) required 83 h to peak age at

165 °C and sample 6 required only 50 h to peak age. Ageing at 180 °C shows the same trends. Sample 1 required 67 h to peak age (compared to 166 h for the SHT sample) and sample 3 required only 40 h to peak age. Sample 4 required 58 h and sample 6 required only 25 h. Ageing at 197 °C reduced the time to peak age to 8 h for all the shock-treated samples, regardless of the number of explosive sheets used. The SHT sample required 50 h. Even though shorter times to peak age can be achieved by ageing at 180 or 197 °C, this effect is diminished by lower hardness values obtained from these samples when compared to the 165 °C ageing. Peak age-hardness values are shown in Table III.

The effects of pulse duration can be studied by comparing samples 1 and 3 (SHT condition), and samples 4 and 6 (AR condition) in Table II. In both cases, an increase in pulse duration (1 sheet to 3 sheets) decreased the time to peak age. When ageing at 165 °C, sample 1 (SHT + 1 sheet) peak aged after 116 h while sample 3 (SHT + 3 sheets) peak aged after 60 h, and sample 4 (AR + 1 sheet) peak aged after 83 h while sample 6 (AR + 3 sheets) peak aged after 50 h. When ageing at 180 °C, sample 1 peak aged after 67 h while sample 3 peak aged after 40 h, and sample 4 peak aged after 58 h while sample 6 peak aged after 25 h. Increased pulse duration had no effect on high-temperature (197 °C) ageing treatment, as mentioned earlier.

The hardness of shock-treated samples follows the same trends of the time to peak just discussed. That is, increased pulse duration generally increased the hardness values obtained from the peak-aged conditions. Slightly higher values are obtained for the low-temperature ageing treatment, 165 °C, than for the 180 and 197 °C heat treatments, as shown in Table III.

3.3. Activation energies

The activation energy can be studied from an Arrehenius type of equation because of the temperature dependence of the phenomenon; this is expressed as [11]

$$r = r_0 e^{-Q/RT}$$

where r is the rate of change, r_0 is a constant, e is the base of the natural logarithm, R is the gas constant (1.987 cal mol^{-1}K^{-1}), T is the absolute temperature (K), and Q is the activation energy (cal mol^{-1} 1 cal = 4.2 J). When the logarithm of the rate is plotted against the reciprocal of the temperature, a straight line is obtained with the slope equal to the value of the activation energy Q [12]. In the present study, two straight lines are obtained, because, the ageing curves have minimal increase of the slope for a given time at a given ageing temperature, after which an abrupt increase of slope up to the peak-aged conditions is seen to occur. The slow increase of slope at the beginning of the curves is assumed, herein, to correspond to an annealing process due to the deformation introduced during the shock treatment, as well as to the "incubation period" for precipitation. Once the residual stresses in the lattice have been relieved and some clustering does occur, the precipitation process takes over and the slope of the curves increases.

Tables IV and V summarize the results for the two temperature ranges being studied, 165–180 °C and 180–197 °C. Table IV shows that the SHT sample (no shock treatment) required 4.99 kcal mol^{-1} for the annealing process Q_1. This low value is to be expected because no cold work was applied to the sample. Samples 1, 2, and 3, which are SHT + ST, had increased energies of 10.24, 15.20, and 12.09 kcal mol^{-1}, respectively. These values show that more energy is required to anneal samples that were cold worked from the shock treatment (or conversely, more energy expenditure is required in the so-called "incubation period" prior to precipitation). Samples 4, 5, and 6, which have increased amounts of cold work because they are in the AR + ST condition, show an increase in activation energy values to 20.70, 19.73, and 22.13 kcal mol^{-1}, respectively. When the ageing treatment is performed at higher temperatures (180–197 °C range),

TABLE III Summary of the peak-hardness values from the respective ageing plots

Sample	Peak hardness (KHN)		
	165 °C	180 °C	197 °C
1	141 ± 4	130 ± 4	133 ± 2
3	140 ± 3	136 ± 1	137 ± 4
4	132 ± 4	129 ± 7	129 ± 3
6	138 ± 4	136 ± 2	137 ± 7
SHT	119 ± 3	142 ± 1	80 ± 4
AR	130 ± 5	122 ± 2	128 ± 5

TABLE IV Summary of activation energies for the 165–180 °C range. Q_1 corresponds to the annealing process and Q_2 corresponds to the precipitation process (1 kcal = 4.1840 kJ)

Sample	Q_1 (± *e.s.d.*)[a] (kcal mol^{-1})	Q_2 (± *e.s.d.*)[a] (kcal mol^{-1})
1	10.24 ± 3.3	24.18 ± 1.9
2	15.20 ± 2.4	24.08 ± 0.7
3	12.09 ± 2.2	21.00 ± 1.2
4	20.70 ± 1.5	9.45 ± 0.9
5	19.87 ± 2.3	9.95 ± 1.1
6	22.13 ± 0.6	8.21 ± 0.2
SHT	4.99 ± 1.9	36.14 ± 1.6

[a]e.s.d. = estimated standard deviation.

TABLE V Summary of activation energies for the 180–197 °C range. Q_1 corresponds to the annealing process and Q_2 corresponds to the precipitation process (1 kcal = 4.1840 kJ)

Sample	Q_1 (± e.s.d.) (kcal mol^{-1})	Q_2 (± e.s.d.) (kcal mol^{-1})
1	26.18 ± 3.1	7.60 ± 1.5
2	21.80 ± 3.8	6.94 ± 0.3
3	25.75 ± 2.4	8.10 ± 0.8
4	31.42 ± 0.3	4.72 ± 2.1
5	32.53 ± 0.8	2.95 ± 1.8
6	30.59 ± 0.5	5.00 ± 1.2
SHT	12.87 ± 0.9	10.26 ± 2.3

the same trend is observed but higher values are obtained as shown in Table V. These higher values of Q_1 suggest that more extensive annealing takes place in these samples (possibly even recrystallization, though no evidence of that was observed), and, as a consequence, strength is reduced and ductility is increased.

Table IV also shows that the SHT sample required 36.14 kcal mol^{-1} for the precipitation process, Q_2. The relatively high value is to be expected because this sample is relatively free of structural defects (dislocations, point defect clusters, etc.) and therefore higher energies are required to initiate the precipitation process. Samples 1, 2, and 3 (SHT + ST) exhibited activation energy decreases to 24.18, 24.08, and 21.00 Kcal mol^{-1}, respectively. These values reflect an increase in defect structure caused by the shock treatment, which reduced the energy required for the precipitation process. Samples 4, 5, and 6, which have increased amounts of cold work (AR + ST), show a further decrease in precipitation activation energies to 9.45, 9.95, and 8.21 Kcal mol^{-1}, respectively. The effect of higher ageing temperatures on Q_2 are shown in Table V. In this case, lower values of Q_2 are obtained when ageing at higher temperatures than at lower temperatures. As mentioned before, high ageing temperature reduces dislocation density (and structural defects in general) and, as a result, fewer precipitation sites are available; the increased diffusion rates, however, must more than compensate for this and thus facilitate precipitation of the strengthening phases. In addition, it is also possible that, at high ageing temperatures, precipitation of these phases starts to take place during the annealing, reducing the required energy for the precipitation process.

The precipitation activation energies, Q_2, calculated here represent the activation energies for growth during ageing. It is considered that nucleation occurs early in the ageing process or even during quenching of the samples. Several authors [7, 13] have reported nucleation of the $\delta'(Al_3Li)$ during quenching. Therefore, it can be considered that the activation energies calculated here correspond to the growth of the $\delta'(Al_3Li)$, the $S(Al_2CuMg)$, and the $T_1(Al_2CuMg)$, which are the strengthening phases of this alloy.

Figs 3 and 4 summarize the previous results in plots of Q_2/Q_1 ratio versus number of explosive sheets (pulse duration). This ratio is a measure of how much of the total activation energy ($Q_1 + Q_2$) corresponds to the annealing process, Q_1, and how much corresponds to the precipitation process, Q_2.

Fig. 3 shows that more energy is used for the precipitation process in the case of SHT + ST samples than that of the AR + ST samples. This figure also shows that the ratio for the SHT sample is considerably higher than that for the SHT + ST samples, which is to be expected as explained above.

Fig. 4 shows that, at higher temperatures, the Q_2/Q_1 ratio is still higher for SHT + ST samples than for the AR + ST samples. However, the ratios themselves are very small, which suggests that, when ageing is performed at high temperature, more energy is used for annealing than for precipitation.

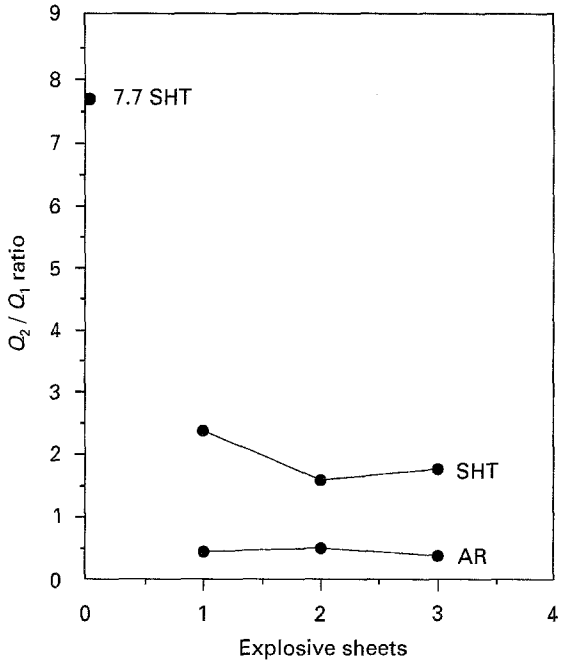

Figure 3 Q_2/Q_1 ratio for the 165–180 °C range.

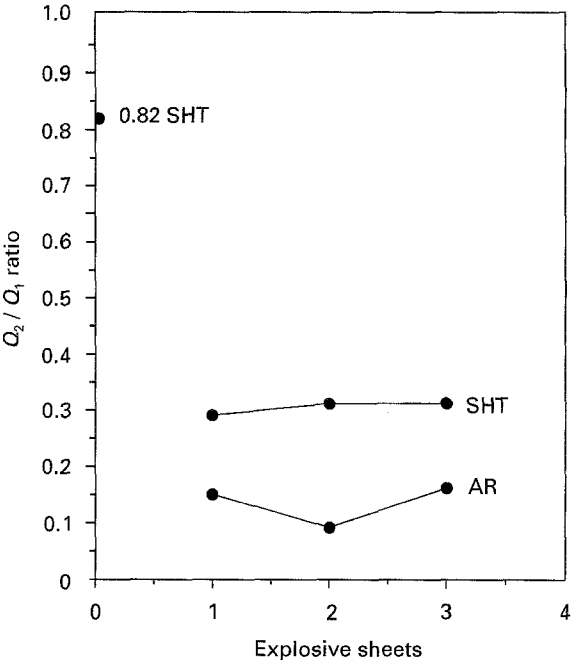

Figure 4 Q_2/Q_1 ratio for the 180–197 °C range.

3.4. Tensile test

Tensile test results are shown in Tables VI–IX. Per cent elongation, 0.2% yield strength, and ultimate tensile strength (UTS) values were measured.

Per cent elongation for SHT + ST samples (samples 1 and 3) that had not been aged is of the order of 9%. In this case, no significant precipitation has taken place, and the material is still relatively ductile. When these samples are peak aged at 165 °C, the elongation decreases to about 4%. Yield strength and UTS values are maximum, suggesting that precipitation of the $S(Al_2CuMg)$ phase has taken place, promoting planar slip. At 197 °C, elongation increases again to about 8% and both yield strength and UTS decrease. These

TABLE VI Summary of tensile test results for the samples that had no ageing heat treatment

Sample	% elongation (cm cm^{-1})	0.2% yield (MPa)	UTS (MPa)
1	9.0 ± 1	176 ± 8	245 ± 7
3	8.0 ± 2	203 ± 5	239 ± 10
4	5.5 ± 1	254 ± 14	356 ± 11
6	3.5 ± 1	275 ± 9	327 ± 8
SHT	28.0 ± 2	115 ± 2	222 ± 2
AR	4.0 ± 2	273 ± 3	333 ± 4

TABLE VII Summary of tensile test results for the samples that were peak aged at 165 °C

Sample	% elongation (cm cm^{-1})	0.2% yield (MPa)	UTS (MPa)
1	3.7 ± 1	372 ± 8	465 ± 9
3	4.4 ± 2	397 ± 5	467 ± 12
4	5.7 ± 1	321 ± 5	411 ± 4
6	5.5 ± 3	328 ± 4	430 ± 2
SHT	9.0 ± 1	307 ± 6	408 ± 6
AR	6.8 ± 1	284 ± 12	379 ± 10

TABLE VIII Summary of tensile test results for the samples that were peak aged at 180 °C

Sample	% elongation (cm cm^{-1})	0.2% yield (MPa)	UTS (MPa)
1	4.0 ± 1	349 ± 9	399 ± 5
3	3.1 ± 1	359 ± 2	405 ± 1
4	3.2 ± 2	333 ± 7	400 ± 8
6	5.9 ± 1	409 ± 5	458 ± 3
SHT	6.6 ± 2	294 ± 1	384 ± 7
AR	4.6 ± 1	313 ± 3	401 ± 4

TABLE IX Summary of tensile test results for the samples that were peak aged at 197 °C

Sample	% elongation (cm cm^{-1})	0.2% yield (MPa)	UTS (MPa)
1	8.5 ± 2	280 ± 3	372 ± 11
3	6.5 ± 1	318 ± 8	379 ± 15
4	6.5 ± 1	314 ± 1	399 ± 2
6	4.5 ± 1	336 ± 2	401 ± 1
SHT	8.5 ± 3	289 ± 10	365 ± 14
AR	6.0 ± 2	295 ± 12	383 ± 7

high ageing temperatures encourage precipitates to grow and to be spaced further apart, so that their effectiveness in stoppage of slip is decreased. Consequently, strength is decreased and ductility increased.

Samples in the AR + ST condition do not follow the above trend. These samples, in contrast, maintain a constant 6% (on average) elongation regardless of the peak-ageing temperature. These results suggest that the amount of strain induced in these samples retards the precipitation of the S(Al_2CuMg) phase. Consequently, the elongation values coincide with those of the underaged treatment.

The SHT sample showed 28% elongation, which is expected, because no appearance of strengthening phases has yet taken place.

Low ductility is associated with the shearable nature of the δ′(Al_3Li) precipitate that forms during ageing, and the presence of precipitate-free zones at high- and low-angle *grain* boundaries; both of these occurrences lead to strain localization [14]. Ductility of the SHT samples is improved upon shock treatment and ageing because of a more homogeneous distribution of the S(Al_2CuMg) and T_1(Al_2CuLi) phases. In addition, the shock treatment decreases the effects of PFZ because it enhances precipitation in the matrix.

A summary of the peak values for the 0.2% yield strength is shown in Table X. It can be seen that for the SHT sample and for the SHT + ST samples (1 and 3), peak values are obtained at 165 °C, whereas for the AR samples and for the AR + ST samples, peak values are obtained at 180 °C. These data seem to confirm the fact that the amount of strain induced in these samples retarded precipitation of the S(Al_2CuMg) phase; therefore higher temperatures were necessary for its precipitation.

The effects of pulse duration, analogous to those observed in the microhardness tests, are also shown in Table X. At 180 °C, sample 1 (SHT + 1 sheet) showed a peak yield strength of 349 MPa, whereas sample 3 (SHT + 3 sheets) showed a peak yield strength of 359 MPa. A similar trend is observed for sample 4 (AR + 1 sheet), which peaked at 333 MPa, and sample 6 (AR + 3 sheets), which peaked at 409 MPa. Similar trends are observed for the non heat-treated samples as well as for the samples heat treated at 165 and 180 °C.

The maximum value of 0.2% offset yield strength, 409 MPa, is observed in sample 6 (AR + 3 sheets) aged at 180 °C. This suggests that the S(Al_2CuMg) phase indeed contributes to the maximum strength observed in this alloy, as reported by Welpman [15].

TABLE X Peak values for 0.2% yield strength

	0.2% yield strength (MPa)					
	1	3	4	6	SHT	AR
No HT	176 ± 8	203 ± 5	254 ± 14	275 ± 9	115 ± 2	273 ± 3
165 °C	372[a] ± 8	397[a] ± 5	321 ± 5	328 ± 4	307[a] ± 6	284 ± 12
180 °C	349 ± 9	359 ± 2	333[a] ± 7	409[a] ± 5	294 ± 1	313[a] ± 3
197 °C	280 ± 3	318 ± 8	314 ± 1	336 ± 2	289 ± 10	295 ± 12

[a] Peak values.

TABLE XI UTS peak values

	Peak UTS (MPa)					
	1	3	4	6	SHT	AR
No HT	245 ± 7	239 ± 10	356 ± 11	327 ± 8	222 ± 2	333 ± 4
165 °C	465[a] ± 9	467[a] ± 12	400 ± 4	430 ± 8	408[a] ± 6	379 ± 10
180 °C	399 ± 5	405 ± 1	411[a] ± 8	458[a] ± 2	384 ± 7	401[a] ± 4
197 °C	372 ± 11	379 ± 15	399 ± 2	401 ± 1	365 ± 14	383 ± 7

[a] Peak values.

A summary of values of ultimate tensile strength (UTS) is shown in Table XI. The SHT and the SHT + ST samples show maximum UTS values when aged at 165 °C. The AR and AR + ST samples show maximum UTS values when aged at 180 °C. This trend is similar to the behaviour observed above.

The effects of pulse duration on the UTS are similar to those on the 0.2% yield strength; that is, at 180 °C, UTS for sample 1 is 399 MPa, but for sample 3 it is 405 MPa. In the case of AR and AR + ST samples, UTS for sample 4 is 400 MPa, whereas that for sample 6 is 458 MPa. Similar trends were observed for the non-heat-treated samples, as well as for those heat treated at 165 and 197 °C.

Two more trends can be observed in Tables X and XI. First, a decrease in the ageing temperature is seen to increase yield strength and UTS values in SHT samples. Second, samples that were SHT before the shock treatment generally have higher yield strength and UTS values than the samples that were shock-treated in the AR condition.

In the first case, increased values of yield strength and UTS with decreasing ageing temperature may be due to the reduction of critical particle radius necessary to provide stable nucleation sites for the $S(Al_2CuMg)$ and $T_1(Al_2CuLi)$ phases, as suggested by Ashton *et al.* [16]. In addition, because smaller radii are needed, the density of nucleation sites is increased. The final result is that these two strengthening phases precipitate in a smaller and more homogeneously distributed form, throughout the material, thus increasing strength.

In the second case, solution heat treatment redissolves all the precipitates formed during the manufacturing process. The post-shock treatment promotes a high density of nucleation sites because dislocation density is increased, and the $S(Al_2CuMg)$ and $T_1(Al_2CuLi)$ phases precipitate preferentially on them due to their large coherency strains [16]. The shock treatment of AR samples slightly increases the strength values, but not as much as in the SHT samples. This increase is due to the fact that precipitates are already formed during the fabrication process, leaving little excess solute still in solution that can produce further precipitates after the shock treatment.

Results from the tensile tests suggest that yield strength and UTS are improved by shock treatment prior to the ageing, confirming the fact that an increase in dislocation density increases the nucleation sites for precipitation of the $S(Al_2CuMg)$ and $T_1(Al_2CuLi)$ phases. Lower ageing temperature also increases strength by increasing nucleation and reducing the critical particle radius needed for stable nuclei.

4. Conclusions

1. The precipitation temperatures for GP zones and $\delta'(Al_3Li)$ are increased by increased cold work (SHT versus AR) present in samples prior to shock treatment in the alloy studied. The precipitation of $S(Al_2CuMg)$ on the other hand, does not seem to be a function of cold work (SHT versus AR) prior to shock treatment.

2. The precipitation temperature for $S(Al_2CuMg)$ phase is seen to decrease with shock treatment of 8090 alloy. This effect could be advantageous in the processing of the Al-8090 alloy, in terms of reducing ageing temperature, and thus avoiding the emergence of the $\delta'(Al_3Li)$ phase.

3. Increased pulse duration is seen to decrease the time to peak age and increase hardness at both 165 and 180 °C, but produces no effect on ageing at 197 °C.

4. The activation energies calculated here suggest that two processes are occurring during the ageing treatment: annealing, Q_1, and precipitation, Q_2. Q_1 increases but Q_2 decreases, as cold work is increased in the material, when ageing is performed in the low-temperature range.

5. The high values of Q_1 obtained when ageing is performed at the higher temperature range (180–197 °C) are estimated to be the result of extensive annealing required. Lower values of Q_2 are estimated to be due to early and easy precipitation during the high-temperature ageing treatment because of the increased rate of diffusion.

6. SHT + ST samples show minimum tensile elongation and maximum yield strength when peak aged at 165 °C, suggesting that $S(Al_2CuMg)$ phase has precipitated, producing planar slip.

7. AR + ST samples show a constant 6% maximum tensile elongation for all the ageing temperatures. Peak yield-strength values are produced at 180 °C, suggesting that $S(Al_2CuMg)$ phase precipitation is retarded because of the extra deformation.

8. An increase in pulse duration increases yield strength and UTS in both AR and SHT shock-treated samples.

Acknowledgements

Partial support for this research was supplied by generous donations from Alcoa Laboratories and Alcoa Foundation and are gratefully acknowledged.

References

1. P. J. BISCHLE and J. W. MARTIN, in "Proceedings of the 4th International Conference on Al-Li", edited by G. Champier and B. Dubost (Les Editions, Paris, France, 1987) p. 761.
2. A. F. SMITH, *ibid*, p. 49.
3. M. NUNOMI and K. DEGAWA, *ibid.* p. C3–653.
4. A. POLATO, in "Proceedings of the 12th Annual Symposium on Behavior and Utilization of Explosives in Engineering Design", edited by L. Davison, J. E. Kennedy and F. Coffey (ASME, Alburquerque, NM, 1972) p. 25.
5. E. A. STARKE and T. H. SANDERS, *J. Metals* **33** (1981) 24.
6. A. K. MUKHOPADHYAY, C. N. TITE, H. M. FLOWER, P. J. GREGSON and F. SALE, in "Proceedings of the 4th International Conference on Al–Li", edited by G. Champier and B. Dubost (Les Editions, Paris, France, 1987) p. 439.
7. S. AVIS, E. EVANGELISTA, P. MENGUCCI and G. RIONTINO, *ibid.*, p. 447.
8. W. S. MILLER, J. WHITE and D. J. LLOYD, *ibid.* p. 447.
9. S. SURESH and A. K. VASUDEVAN, in "Proceedings of the 3rd International Al–Li Conference", edited by T. Sheppard (Institute of Metals, London, 1986) p. 595.
10. L. E. MURR, O. T. INAL and A. A. MORALES, *Acta Metall.* **24** (1985) 268.
11. ALFRED H. GEISLER, "Phase transformations at interfaces" (ASM, Cleveland, OH, 1952), p. 269.
12. DONALD R. ASKELAND, "The science and engineering of materials" (PWS–Kent Co, Boston, MA, 1989) p. 118.
13. J. WHITE, W. S. MILLER, I. G. PALMER, R. DAVIS and T. S. SAINI, in "Proceedings of the 3rd International Al–Li Conference", edited by T. Sheppard (Institute of Metals, London, 1986) p. 425.
14. R. F. ASHTON, D. S. THOMPSON, E. A. STARKE and F. S. LIN, in "Proceedings of the 3rd International Al–Li Conference", edited by T. Sheppard (Institute of Metals, London, 1986) p. 66.
15. K. WELPMAN, M. PETERS, T.H. SANDERS, *ibid.*, p. 524.
16. R. F. ASHTON, D. S. THOMPSON, E. A. STARKE and F. S. LIN, *ibid.*, p. 74.

Received 22 December 1993
and accepted 7 June 1995